

# ESTIMATION OF THE STAR FORMATION RATE USING LONG-GAMMA RAY BURST OBSERVED BY SWIFT

M. Elías,<sup>1</sup> O. M. Martínez,<sup>1</sup>

*Draft version: June 8, 2020*

## RESUMEN

En este trabajo se estima la Tasa de Formación Estelar (SFR) mediante el análisis de una muestra de 333 *Gamma Ray Bursts* (GRBs) Largos detectados por Swift. Este estudio se basa en el modelo empírico propuesto por Yüksel et al. (2008), básicamente, la SFR se calcula utilizando GRBs Largos tomando en consideración que son originados según el modelo Collapsar o del colapso de estrellas masivas tipo hipernova ( $M > 20M_{\odot}$ ). El análisis parte del estudio de  $\varepsilon(z)$  que representa la tasa de producción de GRBs Largos, parametrizándolo de la forma  $\varepsilon(z) = \varepsilon_0(1+z)^{\delta}$ , donde  $\varepsilon_0$  incluye la conversión absoluta de la SFR a la tasa de GRB en un rango de luminosidad de GRB dado y el índice  $\delta$  es un parámetro dinámico que cambia con  $z$  y representa la pendiente de la traza dejada por la SFR. Los resultados favorecen la propuesta usar a los GRBs Largos como trazadores de la SFR.

## ABSTRACT

In this work we estimate the Star Formation Rate (SFR) through 333 Long-GRBs detected by Swift. This investigation is based on the empirical model proposed by Yüksel et al. (2008), basically, the SFR is estimated using long-GRBs considering that they have an stellar origin based on the Collapsar model or the collapse of massive stars (Hypernova)  $M > 20M_{\odot}$ . The analysis starts with the study of  $\varepsilon(z)$  which accounts the long-GRBs production rate and it is parameterized by  $\varepsilon(z) = \varepsilon_0(1+z)^{\delta}$  where  $\varepsilon_0$  include the SFR absolute conversion to GRBs rate in a luminosity range already defined and  $\delta$  is a dynamical parameter which changes at different regions of redshift it accounts the SFR slope which is obtained by an analysis of linear regression over our Long-GRBs sample, the results obtained provide evidence that support our proposal to use Long-GRBs as tracers of SFR.

*Key Words:* galaxies: star formation — gamma-ray burst: general — stars: massive

## 1. INTRODUCTION

Gamma Ray Burst are related to extremely energetic explosions in far away galaxies (for reviews, see Wang et al. (2015); Wei & Wu (2017); Petitjean et al.

---

<sup>1</sup>Benemérita Universidad Autónoma de Puebla

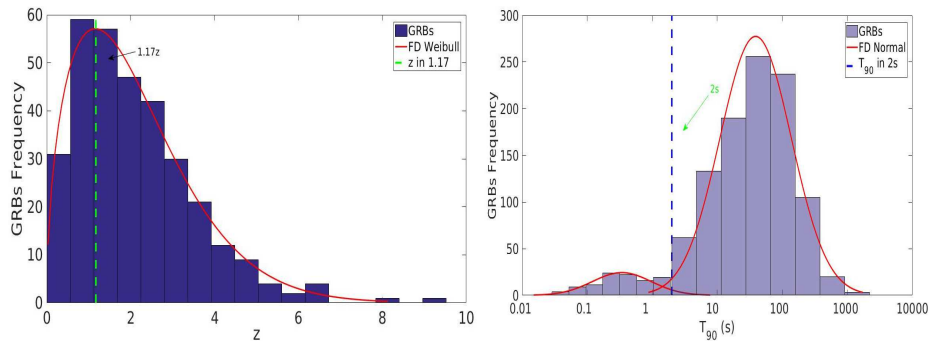


Fig. 1. **Left** Frequency histogram of 333 Long-GRBs over  $z$  where the data presents its mode at  $1.17z$  and mean at  $z = 2.06$  these results match with the observational results. **Right** Bimodal distribution of our sample made up by 994 Long-GRBs where we can see both types of GRBs (Long  $T_{90} > 2s$  and Short  $T_{90} < 2s$ )

(2016) ), based on the collapse model which proposes the formation of Long-GRBs by the collapse of rapidly rotating super massive star (e.g. Wolf-Rayet star  $M > 20M_{\odot}$ , for cosmological implications of GRBs see Wei & Wu (2017))

we can trace and prove the SFR (Yüksel et al. 2008) (Kistler et al. 2008) (Wang 2013) related with this events. The study of SFR through traditional tracers as continuous UV (Cucciati et al. 2012), (Schenker et al. 2013), (Bouwens et al. 2014), recombination lines of:  $H\alpha$ , Far Infrared (Magnelli et al. 2013), (Gruppioni et al. 2013), radio emission and X-ray, are inefficient at high redshift ( $z > 4$ ) (Schneider 2015) due for their sensitivity to extinction for gas and dust and the universe expansion.

The stellar formation activity in the universe was very intense in the past, higher than now, in  $z \sim 2.5$  about 10% of all stars were formed and about 50% of the local universe took place in  $z \sim 1$ , (Schneider 2015) , the star formation rate density is a function which evolves with the time, it has shown an increase of 10 times bigger between now and  $z \sim 1$  holding until  $z \sim 3 - 4$  and finally it decreases at  $z > 4$  (Hopkins & Beacom 2006)(Carroll & Ostlie 2006) (Schneider 2015) , the figure 1 show the distribution of our sample with the redshift, where the data presents a mode at  $z \approx 1.17$  and mean at  $z \approx 2.06$  these results match with the observational results.

The paper is organized as follows. In §2 we present the main properties of our Long-GRBs sample. In §3 we develop the mathematical model to calculate the SFR using Long-GRBs as a tracers. In §4 we present the results based on the compute of  $\delta$  obtained by an analysis of linear regression over the Long-GRB sample. We conclude in §5.

## 2. DESCRIPTION OF THE SAMPLE

The data sample used, includes 959 GRBs observed by Swift supplied by Butler et al. (2017) and 35 bursts detected by FERMI from Singer et al.

(2015), BeppoSAX from Frontera et al. (2009) and ROTSE from Rykoff et al. (2009) obtaining a total of 994 GRBs, where 333 are Long-GRBs with  $T_{90}$  and  $z$  established, from these 333 only 263 presents an isotropical Energy  $E_{iso}$  already defined. We consider bursts up to 2017 June 4, the fig 1 shows the data considered, as it was observed by BATSE the bimodal distribution allow to define the short and Long-GRBs.

### 3. DERIVATION OF THE SFR USING GRBS

The conversion factor between GRBs rate and SFR is hard to identify, supported by an increasing amount of data of the cosmic star formation rate at low redshift  $z < 4$  (Cucciati et al. 2012)(Dahlen et al. 2007)(Magnelli et al. 2013) and the relationship between Long-GRB and star formation based in the hypernova model we can relate the observed GRBs in low redshift with the SFR measurements considering an additional evolution of GRBs rate with SFR (Kistler et al. 2008)(Yüksel et al. 2008).

GRBs distribution per unit of redshift over all sky is giving by

$$\frac{d\dot{N}}{dz} = F(z) \frac{\varepsilon(z) \dot{\rho}_*(z)}{\langle f_{beam} \rangle} \frac{\frac{dV_{com}}{dz}}{1+z} \quad (1)$$

Where  $0 < F(z) < 1$  accounts the probability to obtain the redshift related to afterglow from their host galaxy.  $\varepsilon(z)$  accounts the Long-GRBs rate production with additional evolution effects.  $\langle f_{beam} \rangle$  accounts the number of GRBs that are observed due for their beaming,  $\dot{\rho}_*(z)$  accounts the SFR density where the dot represent comoving coordinate,  $1/(1+z)$  is a factor related to cosmological time dilation.  $dV_{com}/dz$  differential volume in comoving coordinates per redshift unit.  $\varepsilon(z)$  is parameterized as  $\varepsilon(z) = \varepsilon_0(1+z)^\delta$  where  $\varepsilon_0$  is a constant which includes the absolute conversion from SFR to GRB in a GRB luminosity range,  $\delta$  accounts the slope left by the trace of the SFR in a redshift range.

The table 1 presents 10 elements of the sample, listing some spectral properties as **Energy Fluence**<sup>3</sup>, **Peak Energy Flux**<sup>4</sup>, **Peak Energy Flux**<sup>5</sup>  $E_{iso}$ , **Ep** and  $T_{90}$ , using  $E_{iso}$  we can obtain the Isotropical luminosity  $L_{iso}$  by the equation 2

$$L_{iso} = \frac{E_{iso}(1+z)}{T_{90}} \quad (2)$$

In the figure 2 we present the luminosity distribution of our sample made up by 263 Long-GRBs, here we observed the relation between ( $L_{iso}$ ) with redshift considering that only highly luminous GRBs can be seen in high  $z$ , using a luminosity boundary of  $L_{iso} > 10^{51} \text{ergs}^{-1}$  established by Kistler et al.

<sup>2</sup> the comoving volume is giving by  $dV_{com}/dz = 4\pi D_{com}^2 * dD_{com}/dz$   
the comoving distance  $dD_{com}$  is giving by  $dD_{com} = c/H_0 \int_0^z dz' (\Omega_m (1+z')^3 + \Omega_\Lambda)^{-1}$   
<sup>3</sup> (15 – 150 keV) [erg cm<sup>-2</sup>]  
<sup>4</sup> (15 – 150 keV) [erg cm<sup>-2</sup> s<sup>-1</sup>]  
<sup>5</sup> (15 – 150 keV) [ph cm<sup>-2</sup> s<sup>-1</sup>]

N	GRB	$z$	$T_{90}$	Ep [keV]	Energy Fluence	Peak Energy Flux	Peak Photon Flux	$E_{iso}$ [erg]
1	GRB140512A	0.73	158.76	270.4481	1.29E-05	5.69E-07	7.09467	5.47E+50
2	GRB140518A	4.71	61.32	46.5668	1.04E-06	5.38E-08	0.88978	4.98E+51
3	GRB141225A	0.92	40.77	132.6695	2.59E-06	1.06E-07	1.27368	3.86E+51
4	GRB150301B	1.52	13.23	106.8910	1.81E-06	2.14E-07	2.82063	1.14E+52
5	GRB150323A	0.59	150.4	81.3815	5.40E-06	2.98E-07	4.42309	9.30E+49
6	GRB150403A	2.06	38.28	227.8612	1.58E-05	1.48E-06	17.2206	3.07E+52
7	GRB150413A	3.14	264.29	63.1096	4.50E-06	6.83E-08	0.986981	5.04E+51
8	GRB150818A	0.28	134.39	74.8740	3.97E-06	1.12E-07	1.71705	3.31E+49
9	GRB150821A	0.76	149.93	197.5467	2.18E-05	4.24E-07	5.02955	5.70E+51
10	GRB151029A	1.42	9.28	31.3418	4.15E-07	8.87E-08	1.71218	9.01E+50

TABLE 1

## SPECTRAL PROPERTIES OF THE SAMPLE.

(2008), the spatial distribution of the events are in 5 redshifts bins 1 – 4, 4 – 5, 5 – 6, 6 – 8 and 8 – 10 where we will calculate the SFR

The theoretical accounts of GRBs in the range of redshift from 1 to 4 are expressed by the equation 3 <sup>6</sup>.

$$N_{1-4}^{teo} = \Delta t \frac{\Delta\Omega}{4\pi} \int_1^4 dz F(z) \varepsilon(z) \frac{\dot{\rho}_*(z)}{\langle f_{beam} \rangle} \frac{dV_{com}}{dz} \frac{1}{1+z}$$

$$N_{1-4}^{teo} = A \int_1^4 dz \dot{\rho}_*(z) (1+z)^\delta \frac{dV_{com}}{dz} \frac{1}{1+z} \quad (3)$$

Where

$$A = \frac{\Delta t \Delta\Omega F(z) \varepsilon_0(z)}{4\pi \langle f_{beam} \rangle}$$

A depends in the total observed time by Swift  $\Delta t$  and the angular sky coverage  $\Delta\Omega$ , utilizing the SFR overage density  $\langle \dot{\rho}_* \rangle_{z_1-z_2}$  we compute the theoretical accounts of GRB in a range of redshift from  $z_1$  to  $z_2$  is given by

$$N_{z_1-z_2}^{teo} = \langle \dot{\rho}_* \rangle_{z_1-z_2} A \int_{z_1}^{z_2} dz (1+z)^\delta \frac{dV_{com}}{dz} \frac{1}{1+z} \quad (4)$$

Taking the calculus of GRBs observed  $N_{z_1-z_2}^{obs}$  we obtain the SFR in a specific range of  $z$ ,  $z_1 - z_2$  and using the bin 1 – 4 we determine the SFR overage density in the equation 5

$$\langle \dot{\rho}_* \rangle_{z_1-z_2} = \frac{N_{z_1-z_2}^{obs}}{N_{1-4}^{obs}} \frac{\int_1^4 dz \frac{dV_{com}}{dz} (1+z)^\delta \dot{\rho}_*(z)}{\int_{z_1}^{z_2} dz \frac{dV_{com}}{dz} (1+z)^\delta} \quad (5)$$

## 4. DESCRIPTION OF THE SFR MODEL BY LONG-GRBS

Considering the results obtained by Hopkins & Beacom (2006) and studies made by Yu et al. (2015) about the GRBs rate compared with SFR we defined

<sup>6</sup>we use the values  $\Omega_m = 0.3, \Omega_\Lambda = 0.7$  based on the latest studies of Wilkinson Microwave Anisotropy Probe (WMAP) and Hubble Key Project (HKP) in a flat universe

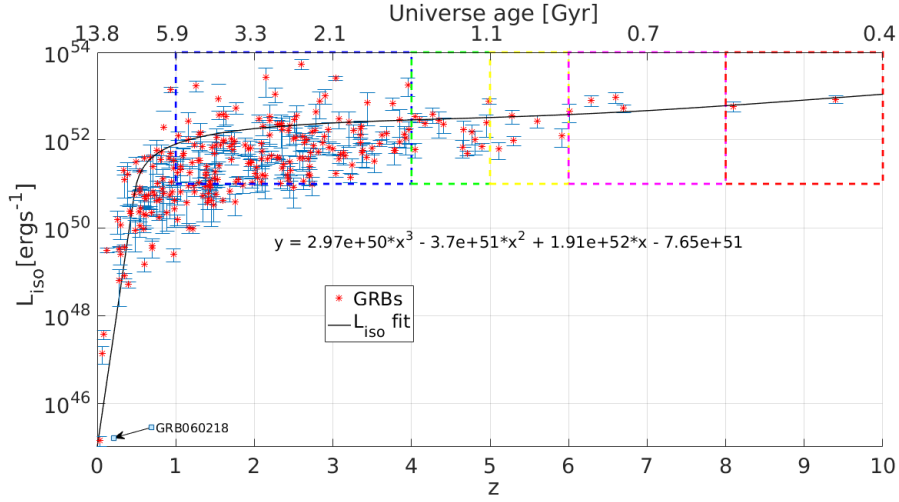


Fig. 2. Distribution of 263 Long-GRBs detected by Swift from Butler et al. (2017), we highlight 5 areas used to estimated the SFR density at different redshift bins (1 – 4, 4 – 5, 5 – 6, 6 – 8, 8 – 10) as discuss in the document, with (173, 15, 4, 2) burst respectively.

the best fit to  $\delta$  in different ranges of  $z$ , where the best fit to  $\dot{\rho}_*$  is giving by the table 2

We calculate  $\dot{\rho}_*(z)$  parameterized as a function of redshift and  $\delta$  using a power law, considering that we are including a bigger range of redshift and also a bigger account of Long-GRBs than Yüksel et al. (2008) we extend their model with the equation 6 adding the term  $\eta$  representing the overage account of Long-GRBs observed in the bin of  $z$  ( $z_1, z_2$ ) normalized by the account of Long-GRBs in the bin (1,4).

$$\dot{\rho}_*(z) = \eta \rho_+(z) = \left(1 + \frac{N_{1-4}^{obs}}{N_{z_1-z_2}(z_1 + z_2)/2}\right) \rho_+(z) \quad (6)$$

where  $\rho_+$  is given by equation 7 proposed by Yüksel et al. (2008), in order not to lose consistency we use  $\rho_+$  as  $\dot{\rho}_*$ .

$$\dot{\rho}_*(z) = \dot{\rho}_0 \left[ (1+z)^{a\tau} + \left(\frac{1+z}{B}\right)^{b\tau} + \left(\frac{1+z}{C}\right)^{c\tau} \right]^{\frac{1}{\tau}} \quad (7)$$

Where the constants  $a, b$  y  $c$  includes the logarithmic slope  $\delta$  of the track left by  $\dot{\rho}_*(z)$  (see table 2), the normalization is  $\dot{\rho}_0 = 0.02 M_{\odot} yr^{-1} Mpc^{-3}$  and  $\tau \approx -10$ . ( see Yüksel et al. (2008) for more details), we defined  $A$  y  $B$  with the next expressions

$$B = (1 + z_1)^{1 - \frac{a}{b}}$$

$$C = (1 + z_1)^{\frac{b-a}{c}} (1 + z_2)^{1 - \frac{b}{c}}$$

our first approximation of the density  $\dot{\rho}_*(z)$ , using the best fit of  $\delta$  from literature (see table 2) is

$$\dot{\rho}_*(z) = 0.02 \left[ (1+z)^{-30} + \left( \frac{1+z}{18.27} \right)^{9.4} + \left( \frac{1+z}{6.61} \right)^{43.6} \right]^{-\frac{1}{10}} \quad (8)$$

In the figure 3 it is shown the  $\sigma$  confidence interval. The version update to the SFR in a specific range of  $z$  of Yüksel et al. (2008) used in this work is described by the next equation.

$$\langle \dot{\rho}_* \rangle_{z_1-z_2} = \frac{N_{z_1-z_2}^{Obs} + \frac{N_{1-4}^{Obs}}{z_1+z_2}}{N_{1-4}^{Obs}} \frac{\int_1^4 dz \frac{dV_{com}}{1+z} (1+z)^\delta \dot{\rho}_*(z)}{\int_{z_1}^{z_2} dz \frac{dV_{com}}{1+z} (1+z)^\delta} \quad (9)$$

#### 4.1. Statistical Analysis of the model

Considering  $\delta$  which accounts the slope left by the trace of the SFR function in a redshift range is not constant and taking account the relation between GRB with an stellar origin by the hypernova model (Schneider 2015)(Carroll & Ostlie 2006) we calculate these  $\delta$ s directly from the sample through linear regression over the  $z$  bins 0 – 1, 1 – 4 and 4 – 10 where every region has 89, 214, and 30 respectively and due that  $z$  has 3 significant digits, we did the analysis using grouped data

We calculate the frequency table of each bin and their respective histogram, which lets us obtain the linear regression over the data, getting their respectively slope, in the bin 0 – 1 with 89 burst we obtain the linear equation  $y = 2.32x + 3.4286$ , in the bin 1 – 4, with 214 burst we obtain the linear equation  $y = -1.0643x + 22.781$  and the bin 4 – 10, with 30 burst we obtain the linear equation  $y = -4x + 18$ . proceeding with the analysis we calculate the confidence interval over one  $\sigma$  of significance, getting the best fit to the model at different ranges of  $z$ , this is shown in the table 2

Based on the results of the statistical analysis we calculate the density  $\dot{\rho}_*(z)$  and the average density  $\langle \dot{\rho}_* \rangle_{z_1-z_2}$ , in the figure 4 we compare the results with the ones obtained by traditional tracers.

## 5. DISCUSSION AND CONCLUSION

In this paper we presented the results of our work based in the estimation of the SFR through a mathematical model which relates GRB directly with an stellar origin. we used the latest Swift catalog supplied by Butler et al. (2017). Based in the distribution of  $L_{iso}$  (see figure 2) we computed the SFR using first the values of  $\delta$  from literature (see figure 3), we made a linear regression analysis with our Long-GRB sample reproducing the reported  $\delta$

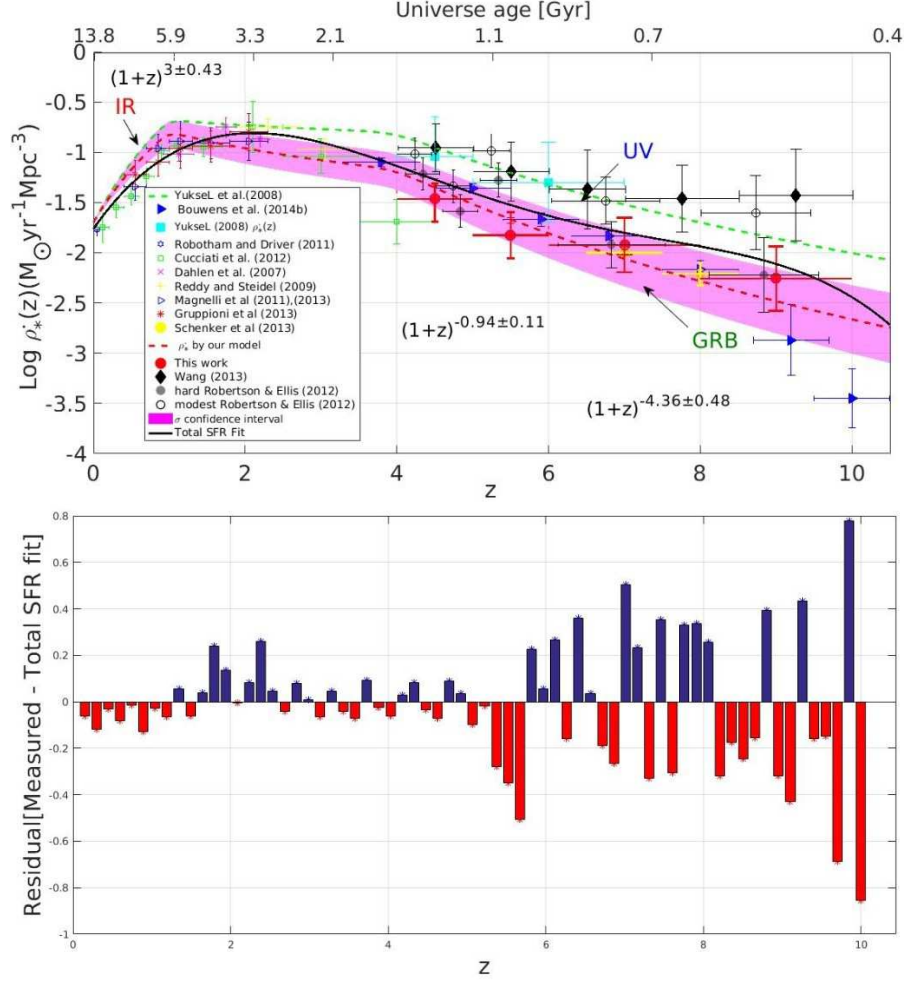


Fig. 3. **Top** Logarithmic distribution of  $\log(\dot{\rho}_*)(z)$  vs redshift where we present the results and comparison between different tracers, the results are plotted in red solid diamonds, and results obtained in UV and FIR are plotted, the wine color region accounts the confidence interval with  $1\sigma$  of significance and the black line represent the total SFR density fit with equation  $\log_{10} \dot{\rho}_* = -0.002z^4 + 0.053z^3 - 0.414z^2 + 1.101z - 1.764$  **Bottom** Residual plot of  $\log(\dot{\rho}_*)(z)$ , we observe significance high dispersion at high redshift  $z > 5$  symmetrical distribution of the data show a good fit to the data.

indexes (see table 2), using these results we compute a new values to SFR average density  $\langle \dot{\rho}_* \rangle_{z_1-z_2}$ . We are including a bigger range of redshift than Yüksel et al. (2008) and a bigger account of Long-GRBs than Wang (2013) we extend the model adding a new term  $\eta$  (see equation 9). our results are compared with the results from traditional tracers as UV and FIR (see figure 4), in contrast to some other results such as Robertson & Ellis (2012) found higher and similar values of  $\dot{\rho}_*$  at  $z > 4$  than ours based in a modest and hard

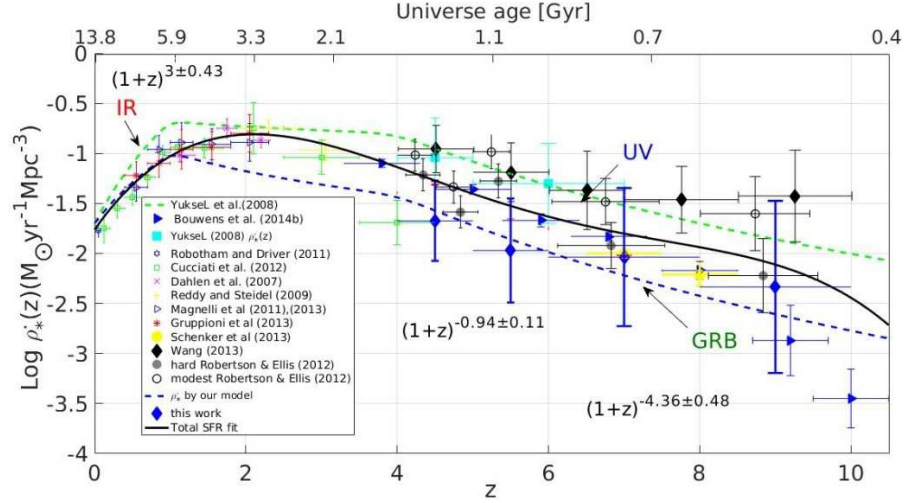


Fig. 4. Logarithmic distribution of SFR  $\log(\dot{\rho}_*)(z)$  vs redshift analogous to the fig 3 where we present the results and comparison between different tracers, our results are plotted in blue solid diamonds using  $\delta$  indexes from our statistical analysis and the black line represent the total SFR density fit

Reference	Redshift range	$\text{Log}(\dot{\rho}_*), [M_{\odot} \text{yr}^{-1} \text{Mpc}^{-3}]$	symbol in figure 3, 4
This work ( $\delta$ proposed)	4-5	-1.47	red solid diamond
	5-6	-1.87	
	6-8	-1.92	
	8-10	-2.26	
This work ( $\delta$ calculated)	4-5	-1.67	blue solid diamond
	5-6	-1.97	
	6-8	-2.04	
	8-10	-2.33	
Redshift bins		$\delta$ proposed	$\delta$ calculated
0	1	$3 \pm 0.43$	$2.3 \pm 0.8$
1	4	$-0.94 \pm 0.11$	$-1.1 \pm 0.2$
4	10	$-4.36 \pm 0.48$	$-4 \pm 1.8$

TABLE 2

SUMMARIZE BETWEEN DIFFERENT VALUES OF THE SFR  
OBTAINED BY THIS WORK.

evolution of the SFR with  $\delta = 0.5$  and  $\delta = 1.5$  respectively considering GRBs from low metallicity host galaxies with  $12 + \log[O/H] \approx 8.7$  (Savaglio et al. 2005) Their results with  $\delta = 0.5$  and  $\delta = 1.5$  are shown as open black circles and solid gray circle in figure 3 and 4 Our results can be marginally consistent with the gray circles. Wang (2013) used a sample of 110 luminous Swift GRBs to find an index value of  $\delta \approx 0.5$  based on the origin of GRBs produced by rapidly rotating metal-poor stars with low mass, their SFR is higher than our



results. This may be a consequence for the update used of the Swift GRB sample in our work and the type of model proposed for the estimation of SFR considering our model highly dependence in the selected index value  $\delta$  at different redshift bins

considering the physical implication and the results obtained along this work we conclude the next points.

- Considering the index  $\delta$  represents the slope due for the SFR trace at different evolution stages of the universe, some previous studies have concluded that star formation dependents based on GRB at high redshift would be sufficient to maintain cosmic reionization over  $6 < z < 9$  (e.g., Yüksel et al. (2008) ; Kistler et al. (2008)). This possibility affect directly in the index value  $\delta$  giving a minimums and maximums values for this parameter when observational results show that GRBs are prompts to appear in low metallicity host galaxies (Savaglio et al. 2005) implying a possible metallicity limits for a massive star to transform into an successful GRB. Concluding that the decreasing of cosmic metallicity may to rise the relative number of GRBs at high redshift and decrease to the local universe (Butler et al. 2017) this observational results constrain the values of  $\delta$  obtained by our model using regression analyses over our GRBs Swift sample.
- The figure 1 the frequency histogram of frequency distribution of 333 Long-GRBs with redshift show a Weibull distribution with mode at  $z \approx 1.17$  and mean at  $z \approx 2.06$ . these values match with observational results of SFR , considering that in  $z \sim 2.5$ , about 10% of all stars were formed and about 50% of the local universe took place at  $z \sim 1$ , Schneider (2015).
- We computed the values of the  $\log\langle\dot{\rho}_*\rangle_{z_1-z_2}$  using both values of  $\delta$  from literature and by our linear regression analysis where the best fit to  $\delta$ , it is shown in table 2 our results match with the results from traditional tracers as UV, and FIR, this provide evidence that support our proposal to use Long-GRBs as tracers of SFR.
- The Isotropically luminosity distribution  $L_{iso}$  (see figure 2) presents one particular outlier, the Long-GRB 060218 in  $z = 0.03$  with the lowest  $L_{iso}$  and also the largest  $T_{90}$  ( $\approx 2100s$ ) this atypical values convert this event into a new topic to investigate due for its strange properties.

(Nicastro et al. 2018)

## REFERENCES

- Bouwens, R. J., Bradley, L., Zitrin, A., et al. 2014, ApJ, 795, 126  
 Burrows, D. N., Hill, J. E., Nousek, J. A., et al. 2005, Space Sci. Rev., 120, 165  
 Butler 2017, SWIFT BAT Integrated Spectral Parameters,  
[http://butler.lab.asu.edu/swift/bat\\_spec\\_table.html](http://butler.lab.asu.edu/swift/bat_spec_table.html)

- Carroll, B. W., & Ostlie, D. A. 2006, *An Introduction to Modern Astrophysics*, Wiley, 489 pp.
- Cucciati, O., Tresse, L., Ilbert, O., et al. 2012, *A&A*, 539, A31
- Dahlen, T., Mobasher, B., Dickinson, M., et al. 2007, *ApJ*, 654, 172
- Frontera, F., Guidorzi, C., Montanari, E., et al. 2009, *ApJS*, 180, 192
- Graziani, C. 2011, *MNRAS*, 416, 57
- Gruppioni, C., Pozzi, F., Rodighiero, G., et al. 2013, *MNRAS*, 432, 23
- Hopkins, A. M., & Beacom, J. F. 2006, *ApJ*, 651, 142
- Kistler, M. D., Yüksel, H., Beacom, J. F., & Stanek, K. Z. 2008, *ApJ*, 673, L119
- Madau, P., & Dickinson, M. 2014, *ARA&A*, 52, 415
- Magelli, B., Popesso, P., Berta, S., et al. 2013, *A&A*, 553, A132
- Narayana Bhat, P., Meegan, C. A., von Kienlin, A., et al. 2016, *ApJS*, 223, 28
- Petitjean, P., Wang, F. Y., Wu, X. F., & Wei, J. J. 2016, *Space Sci. Rev.*, 202, 195
- Robertson, B. E., & Ellis, R. S. 2012, *ApJ*, 744, 95
- Robotham, A. S. G., Norberg, P., Driver, S. P., et al. 2011, *MNRAS*, 416, 2640
- Reddy, N. A., & Steidel, C. C. 2009, *ApJ*, 692, 778
- Rykoff, E. S., Aharonian, F., Akerlof, C. W., et al. 2009, *ApJ*, 702, 489
- Savaglio, S., Glazebrook, K., Le Borgne, D., et al. 2005, *ApJ*, 635, 260
- Schenker, M. A., Robertson, B. E., Ellis, R. S., et al. 2013, *ApJ*, 768, 196
- Schneider, P. 2015, *Extragalactic Astronomy and Cosmology: An Introduction*, ISBN 978-3-642-54082-0. Springer-Verlag Berlin Heidelberg, 2015, 489 pp.
- Singer, L. P., Kasliwal, M. M., Cenko, S. B., et al. 2015, *ApJ*, 806, 52
- Wang, F. Y. 2013, *A&A*, 556, A90
- Wang, F. Y., Dai, Z. G., & Liang, E. W. 2015, *MNRAS*, 454, 1
- Wei, J.-J., Hao, J.-M., Wu, X.-F., & Yuan, Y.-F. 2016, *Journal of High Energy Astrophysics*, 9, 1
- Wei, J.-J., & Wu, X.-F. 2017, *International Journal of Modern Physics D*, 26, 1730002
- Yüksel, H., Kistler, M. D., Beacom, J. F., & Hopkins, A. M. 2008, *ApJ*, 683, L5
- Yu, H., Wang, F. Y., Dai, Z. G., & Cheng, K. S. 2015, *ApJS*, 218, 13
- Nicastro, F., Kaastra, J., Krongold, Y., et al. 2018, *Nature*, 558, 406